ACCOUNTS
of chemical research

Profiling Physicochemical Changes within Catalyst Bodies during Preparation: New Insights from Invasive and Noninvasive Microspectroscopic Studies

LETICIA ESPINOSA-ALONSO, ANDREW M. BEALE, AND BERT M. WECKHUYSEN*

Inorganic Chemistry and Catalysis, Debye Institute for Nanomaterials Science, Utrecht University, Sorbonnelaan 16, 3584 CA Utrecht, The Netherlands

RECEIVED ON MARCH 12, 2010

CONSPECTUS

Cylindrical or spherical catalyst bodies with sizes ranging from tens of micrometers to a few millimeters have a wide variety of industrial applications. They are crucial in the oil refining industry and in the manufacture of bulk and fine chemicals. Their stability, activity, and selectivity are largely dependent on their preparation; thus, achieving the optimum catalyst requires a perfect understanding of the physicochemical processes occurring in a catalyst body during its synthesis.

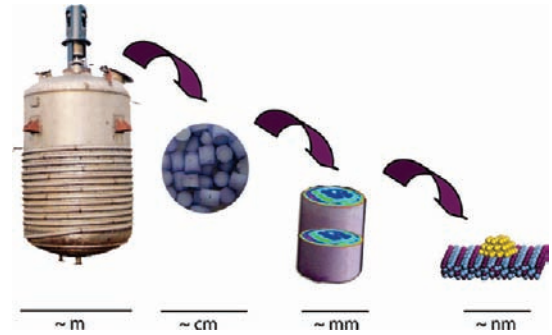

The ultimate goal of the catalyst researcher is to visualize these physicochemical processes as the catalyst is being prepared and without interfering with the system. In order to understand this chemistry and improve catalyst design, researchers need better, less invasive tools to observe this chemistry as it occurs, from the first stages in contact with a precursor all the way through its synthesis. In this Account, we provide an overview of the recent advances in the development of space- and time-resolved spectroscopic methods, from invasive techniques to noninvasive ones, to image the physicochemical processes taking place during the preparation of catalyst bodies.

Although several preparation methods are available to produce catalyst bodies, the most common method used in industry is the incipient wetness impregnation. It is the most common method used in industry because it is simple and cost-effective. This method consists of three main steps each of which has an important role in the design of a catalytic material: pore volume impregnation, drying, and thermal treatment. During the impregnation step, the interface between the support surface and the precursor of the active phase at the solid−liquid interface is where the critical synthetic chemistry occurs. Gas−solid and solid−solid interfaces are critical during the drying and thermal treatment steps. Because of the length scale of these catalyst bodies, the interfacial chemistry that occurs during preparation is space-dependent. Different processes occurring in the core or in the outer rim of the catalytic solid are enhanced by several factors, such as the impregnation solution pH, the metal ion concentration, the presence of organic additives, and the temperature gradients inside the body.

Invasive methods for studying the molecular nature of the metal-ion species during the preparation of catalyst bodies include Raman, UV−vis−NIR, and IR microspectroscopies. Noninvasive techniques include magnetic resonance imaging (MRI). Synchrotron-based techniques such as tomographic energy dispersive diffraction imaging (TEDDI) and X-ray microtomography for noninvasive characterization are also evaluated.

1. Introduction

A large number of industrial catalysts are metals, metal oxides, carbides, and sulfides dispersed on high surface area supports in the presence of various promoters. The support, such as TiO_2, Al_2O_3, SiO_2, or carbon, is a millimeter-sized body that enables a high dispersion of the active phase at

Published on the Web 07/06/2010 www.pubs.acs.org/acr
10.1021/ar100045p

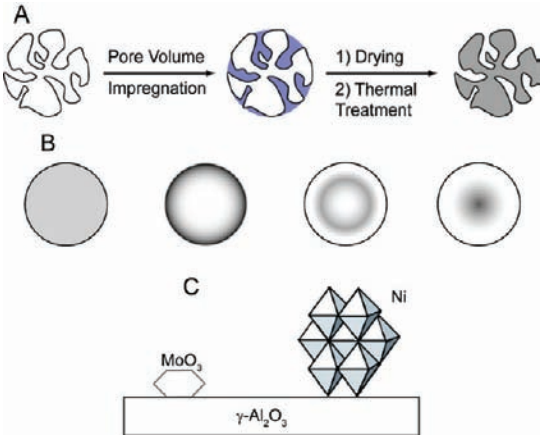

FIGURE 1. (A) Schematic of catalyst preparation via incipient wetness impregnation. The pores of the support appear filled with a solution (blue color) after impregnation. The final catalyst is presented in gray color indicative of the active phase deposited on the support. (B) Different macrodistributions of the active phase (gray) on the support material. (C) Examples of active phases on the support.

high loadings with unique phase−support interactions that result in the required catalytic efficiency (activity, selectivity, and stability). The classical preparation method for industrial catalysts includes incipient wetness impregnation and drying followed by a thermal treatment,[1] as illustrated in Figure 1A. In some cases, an additional activation step is required, such as reduction or sulfidation, to arrive at the active catalytic material. During the incipient wetness impregnation, three phenomena occur: capillary flow of the solution toward the core of the catalyst body, diffusion of the metal ion at the liquid−solid interface, and adsorption of these ions in the pore walls.[2] As a result, depending on the relative importance of each phenomenon, different macrodistributions of the active species along the catalyst bodies can be obtained after impregnation, which can be modified during drying or thermal treatment. In general, four macrodistributions are defined, which are known as uniform, egg shell, egg yolk, and egg white. Figure 1B illustrates the four types of macrodistributions of the active phase within cylindrical catalyst bodies.

Each of the above-mentioned macrodistributions has its own applications, which are generally determined by the reaction kinetics and catalyst poisoning. Uniform macrodistributions are employed if there are no diffusional restrictions, while egg-shell profiles are more favorable in the case of fast reactions. On the other hand, egg-yolk distributions are desired if the external part of the catalyst is exposed to attrition or poisoning, and egg-white can be utilized if the catalyst core suffers diffusional restrictions and the outer rim suffers attrition or poisoning.[2−6] Furthermore, the macrodistributions created during impregnation might be modified by

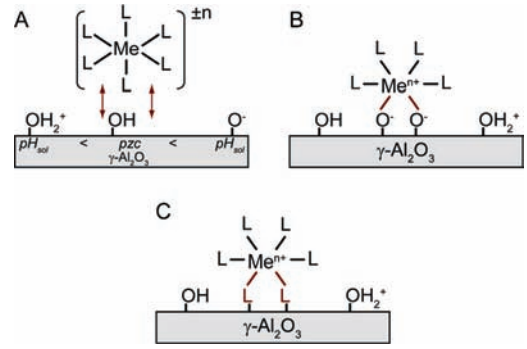

FIGURE 2. Different interactions of a precursor metal-ion complex on a γ-Al_2O_3 surface: (A) electrostatic interactions between the metal-ion complex and the support surface; (B) grafting of the metal-ion complex on the support surface, where two oxygen atoms from the surface enter the 1st coordination sphere of the metal-ion complex; (C) grafting of the metal-ion complex on the support surface through two ligands of the metal-ion complex.

any of the subsequent preparation steps.[2,7] In general, if no physicochemical interactions between the active component and the support surface take place during the impregnation step, then redistribution of the active species occurs unless drying is fast enough to avoid it. An alternative approach to avoid redistribution during drying is increasing the viscosity of the impregnation solution, for example, using aqueous solutions of chelated metal complexes, as described by van Dillen et al.,[8] Negrier et al.,[9] or Ryczkowski.[10] The calcination step, additionally, might lead not only to redistribution of the active component within the catalyst bodies but also to the formation of low dispersions of the active phase or formation of solid solutions with the oxidic support material.[11] As a result, a compromise should be reached among all the experimental parameters (precursor salts and preparation conditions) in order to obtain the optimum catalyst.

Since the support surface contains different types of hydroxyl groups with different acid−base properties, the adsorption of the metal-ion precursor complexes on the support surface is governed by several factors: the point of zero charge (PZC) of the support, solution pH and ionic strength, and nature of the complex, among others, are parameters that can be varied to modify the adsorptive properties of the precursor complex on the support surface.[12] A scheme of the main interactions between a precursor metal-ion complex and γ-Al_2O_3 is presented in Figure 2, where Me refers to the metal, while L and *n* stand for the ligand and the metal-ion (complex) charge, respectively.

Knowledge of the interactions of a precursor metal-ion complex on a support surface can only be obtained by applying spectroscopic characterization techniques. Furthermore, for a real characterization of the preparation of industrial milli-

meter-sized catalysts, the techniques employed must satisfy two requisites. First, they must provide multidimensional information of the structure and composition of a catalyst body, since the size of this material lies in the millimeter range. Second, they must be applied in situ, that is, during the preparation process of the catalyst. In this way, the genesis of the active phase in supported metal oxide catalysts can be monitored and better understood. This Account presents an overview of the different invasive and noninvasive methods currently available with different showcases from our own work to illustrate the advantages of this innovative approach. The Account closes with a look into the future.

2. Invasive Spectroscopic Methods for Catalyst Preparation Studies

Spectroscopy has proven to be a powerful tool for studying the coordination environment of metal-ion complexes at the surface of powdered support materials or crushed catalyst bodies. Still, characterization efforts during catalyst preparation processes are mostly limited to the study of powdered catalysts or crushed catalyst bodies.[13−15] The fundamental but legitimate question that arises is whether the observed physicochemical phenomena for powdered catalysts can be simply extended to millimeter-sized catalyst bodies.

Invasive methods that give information on the molecular nature of the metal-ion species during impregnation, drying, and calcination of catalyst bodies include Raman,[16,17] UV−vis−NIR,[16,18−20] and IR microspectroscopies.[18] The experimental approach to apply these invasive techniques is presented in Figure 3. At different points in time *x* after pore volume impregnation or drying, the catalyst body is bisected perpendicular to its *z* axis using a scalpel. Then, space-resolved spectra can be measured on the resulting cross-section of the catalyst body.

Figure 3 illustrates examples of space-resolved UV−vis−NIR and IR spectra collected along a scan-line of a dried $Ni(en)_3^{2+}/Al_2O_3$ catalyst body, where "en" stands for ethylenediamine.[18] Both the UV−vis and IR spectra show an important spatial variation, with changes in the intensities or positions of the absorption bands, which will have an enormous impact in the final catalyst macrodistribution, as will be explained hereafter.

2.1. UV−vis−NIR Microspectroscopy. UV−vis−NIR spectroscopy allows measurement of the d−d and charge transfer (CT) transitions of various coordination geometries and oxidation states of transition metal-ion complexes as well as the n → π and π → π transitions of organic and inorganic

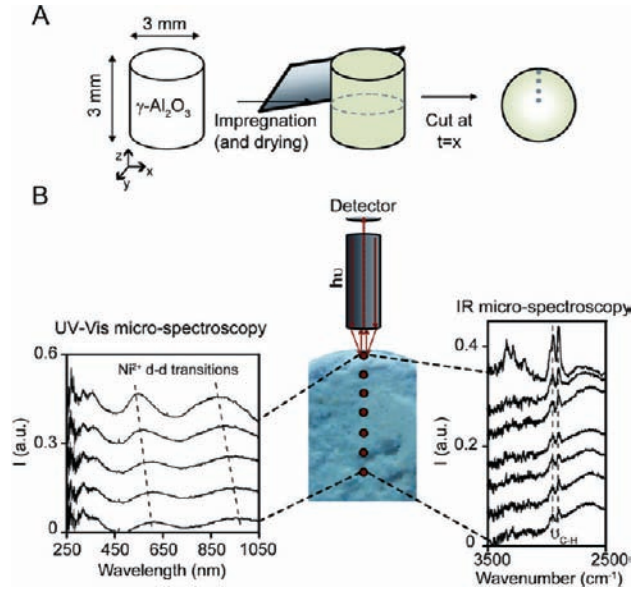

FIGURE 3. (A) Experimental approach when invasive techniques are used to characterize impregnated or dried pellets and (B) example of a bisected pellet together with the spatially resolved UV−vis−NIR and IR spectra collected on the points of the surface indicated in red. The same experimental approach is applied in the case of Raman microspectroscopy.

additives present in the impregnation solutions.[21] The spatial resolution of the currently used experimental setup is on the order of about 200 μm but can be lowered by making some experimental modifications such as varying the distance probe to sample or using optical fibers with smaller diameters (current diameters 100 μm). In addition, this setup makes use of an environmental cell that allows collection of space-resolved spectra immediately after impregnation enabling monitoring of the dynamics of the metal-ion precursor complex.

As an example, this technique was used to understand the role of the support surface on the speciation and dynamics of Ni^{2+} complexes on Al_2O_3 bodies during impregnation. To do so, Al_2O_3 pellets were impregnated with $Ni(en)(H_2O)_4^{2+}$ complexes ("en" = ethylenediamine).

Figure 4A illustrates the UV−vis spectrum of an aqueous solution containing $Ni(en)(H_2O)_4^{2+}$. The spectrum is characterized by a Ni^{2+} d−d transition at 615 nm among others. When this complex is impregnated on powdered Al_2O_3, the UV−vis spectrum of the (just impregnated) wet powder does not change remarkably indicating that the Ni^{2+} complex inside the pores of alumina does not undergo important changes in its molecular structure. However, when the same solution is impregnated on a millimeter-sized Al_2O_3 body, the diffusion of Ni^{2+} toward the core of the catalyst body comes along with changes in its molecular structure (Figure 4B). Five minutes after $Ni(en)(H_2O)_4^{2+}$ is impregnated on a catalyst body, the

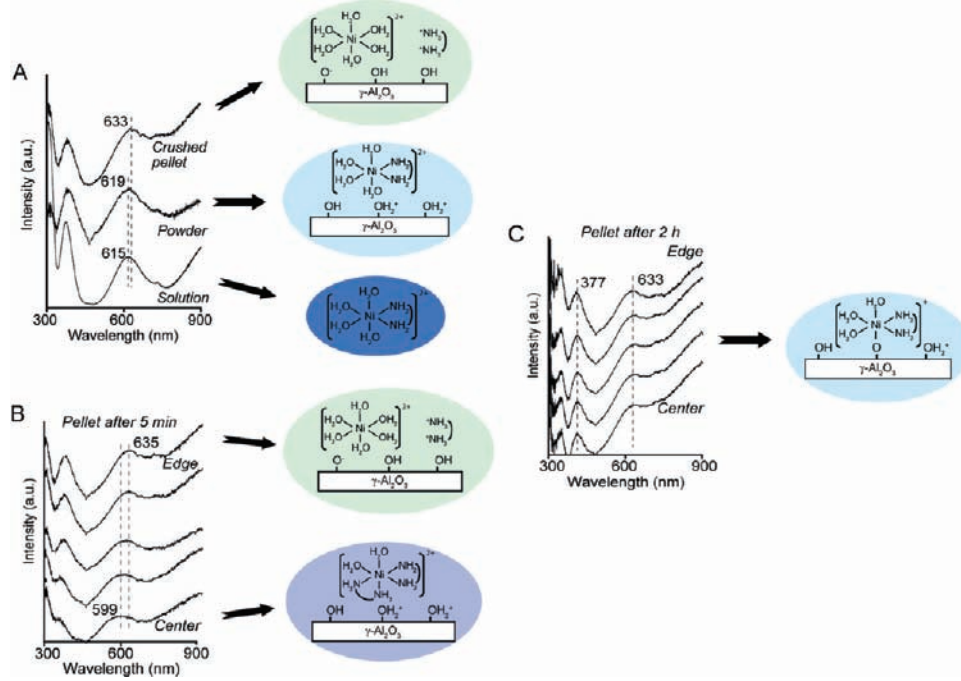

FIGURE 4. (A) UV−vis−NIR spectrum of an aqueous solution containing $Ni(en)(H_2O)_4^{2+}$, together with the corresponding UV−vis−NIR DR spectra obtained after impregnating Al_2O_3 powder or an Al_2O_3 body with the Ni-containing solution. The latter spectrum is obtained after crushing the body. (B, C) Space-resolved UV−vis−NIR spectra of an Al_2O_3 body impregnated with an aqueous solution containing $Ni(en)(H_2O)_4^{2+}$: (B) 5 min and (C) 2 h after impregnation. A schematic of the proposed Ni^{2+} molecular structures deduced from UV−vis (micro)spectroscopy is also presented where the colors correspond to those visually observed.[1,18]

concentration gradient of Ni^{2+} inside alumina causes a strong influence of the support hydroxyl surface on the Ni^{2+} coordination sphere. In the edges, the complex loses its ethylenediamine ligands, as deduced from the red shift of the Ni^{2+} d−d band to 635 nm. This shift is caused by the influence of the acidic hydroxyl groups in the first coordination sphere of the Ni^{2+} complex.[18] However, this influence is temporal, and after 2 h, there is a uniform distribution of Ni^{2+}, as deduced from the identical shape of the UV−vis−NIR spectra along the catalyst body with the Ni^{2+} d−d band centered at 633 nm depicted in Figure 4C. The position of this band suggests either permanent hydrolysis of $[Ni(en)(H_2O)_4]^{2+}$ or a ligand-exchange reaction with the hydroxylic surface of Al_2O_3.[18]

For comparison, an impregnated pellet after five minutes was crushed, and the UV−vis−NIR spectrum is shown in Figure 4A. The maximum absorption appears in between the maximum absorption band recorded in the edge of the catalyst body and that in the center as an average of the spectra collected in all positions inside the catalyst body. This example clearly shows that the behavior of a research catalyst (powder support) during preparation is indeed not identical to that of an industrial catalyst (support body), and therefore, it is crucial to develop space- and time-resolved spectroscopic tools to understand how to prepare industrial catalysts.

2.2. IR Microspectroscopy. IR microspectroscopy is a commercially available technique that can be used to study the vibrational signatures of organic additives, such as amines.[18] Practical spatial resolutions for IR microspectrometers are on the order of 10 μm, but by making use of synchrotron IR light, diffraction-limited spatial resolution of a few micrometers can be reached. However, it is important to stress that due to the low Raman scattering properties of water, Raman microspectroscopy is still beneficial over IR microspectroscopy when aqueous impregnation solutions are applied for catalyst preparation processes. The situation becomes more promising for IR microspectroscopy when dried catalyst bodies are under investigation.

Figure 5 illustrates the space-resolved IR spectra measured on bisected Al_2O_3 bodies after impregnation of $Ni(en)(H_2O)_4^{2+}$, $Ni(en)_2(H_2O)_2^{2+}$, and $Ni(en)_3^{2+}$ complexes and drying of the catalytic materials.[18] IR microspectroscopy in the region between 3500 and 2500 cm^{-1} from the edge to the center of the bisected catalyst bodies reveals several bands: a doublet at approximately 2940 and 2890 cm^{-1} typical of C−H stretching vibrations and, for the sample containing $Ni(en)_3^{2+}$ complexes, two bands at approximately 3330 and 3284 cm^{-1} characteristic of N−H stretching vibrations. These bands come

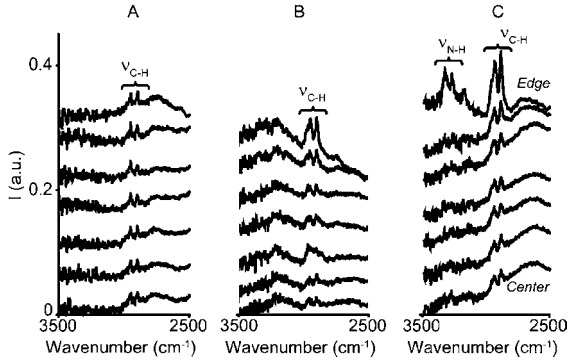

FIGURE 5. Space-resolved IR spectra collected from the edge to the center of dried bisected pellets in the 3500−2500 cm^{-1} region after impregnation with the complexes (A) $Ni(en)(H_2O)_4^{2+}$, (B) $Ni(en)_2(H_2O)_2^{2+}$, and (C) $Ni(en)_3^{2+}$.[18]

from the ethylenediamine ligands coordinating Ni^{2+} in an octahedral symmetry.

From the intensity of the bands in Figure 5A, one can conclude that ethylenediamine was uniformly distributed along the catalyst body when it was impregnated with $Ni(en)(H_2O)_4^{2+}$ complexes and dried, while impregnation and drying of catalyst bodies with $Ni(en)_2(H_2O)_2^{2+}$ and $Ni(en)_3^{2+}$ complexes yielded egg-shell distributions of the organic ligand, as deduced from Figure 5B,C. The macrodistributions of the ligands were verified by UV−vis microspectroscopy and followed the same trend as the macrodistribution of the metal ion.[18] By the combination of IR, UV−vis−NIR, and SEM-EDX space-resolved techniques, it was demonstrated that Ni egg-shell catalysts can be achieved if Ni/en = 1/3 molar ratios are used in the preparation recipe.

2.3. Raman Microspectroscopy. Raman microspectroscopy is commercially available and practical spatial resolutions are around 1−2 μm up to 500 nm, which are mainly determined by the optics of the equipment and the scattering properties of the sample. It can be used to monitor the dynamics and molecular changes of the complex precursors during the wet stage of preparation[22] and also to localize the active phase after drying or calcination.[19,22]

It can be employed, for example, to study the molecular structure of hydrogenated 1 wt % Pd/Al_2O_3 pellets after preparation from aqueous solutions of Na_2PdCl_4 containing different amounts of additional Cl^- ions and different pHs.[19] By tuning these, two different Pd macrodistributions can be achieved. Figure 6 shows the photographs of two bisected pellets after preparation, together with the Raman spectra collected at different positions.

The pellet prepared from the solution containing 94 mM Na_2PdCl_4 and 0.112 M HCl at pH 1 gave rise to a Pd egg-white distribution, and the Raman spectra differ tremendously

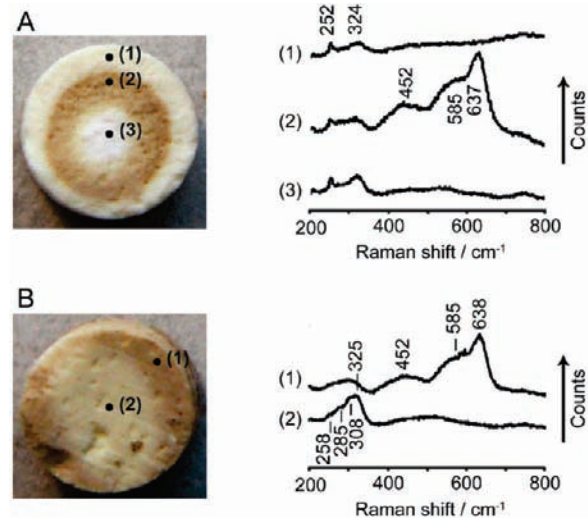

FIGURE 6. Photographs of bisected catalyst bodies after calcination and Raman spectra measured at several points on the bodies. The samples were prepared from (A) 94 mM Na_2PdCl_4/0.112 M HCl at pH 1, and (B) 94 mM Na_2PdCl_4/0.75 M NaCl at pH 5.[19]

depending on the location, as illustrated in Figure 6A. The peaks at 252 and 324 cm^{-1}, which increase in intensity from the edge to the core, are characteristic of the stretching and bending vibrations (Cl−Pd−Cl) of $PdCl_2$ or the ν(Pd−Cl) of $PdCl_4^{2-}$ or its hydrolysis products, suggesting that both the edge and the core of the pellet are rich in chlorinated Pd species. Interestingly, the spectrum in the darker ring shows additionally several broad peaks at 452, 585, and 637 cm^{-1} that can be assigned to PdO or $PdO_{x/2}Cl_{2-x}$. The presence of more oxidic Pd species in this inner ring can also be deduced from the darker color on the photograph.

On the other hand, a brown color was observed in the edge of the pellet prepared from a solution of 94 mM Na_2PdCl_4 and 0.75 M NaCl at pH 5, illustrated in Figure 6B, which agreed with the presence of PdO or $PdO_{x/2}Cl_{2-x}$ deduced from the Raman peaks at 452, 585, and 638 cm^{-1}. Moreover, the core of the pellet showed a broad band centered at around 325 cm^{-1}. The band at 258 cm^{-1} was also measured but its intensity relative to the peak at 325 cm^{-1} was lower than in the previous sample, which suggests the presence of $PdCl_4^{2-}$ or its hydrolysis products with a different Pd structure. This technique indicates there is a speciation of $PdO_{x/2}Cl_{2-x}$ along the catalysts and that Cl^- ions, which can act as a poison for the catalyst, cannot be completely removed from the catalyst during the calcination step.

3. Noninvasive Spectroscopic Methods for Catalyst Preparation Studies

The disadvantage of invasive methods is that bisection of the samples before measurement is a must to obtain information

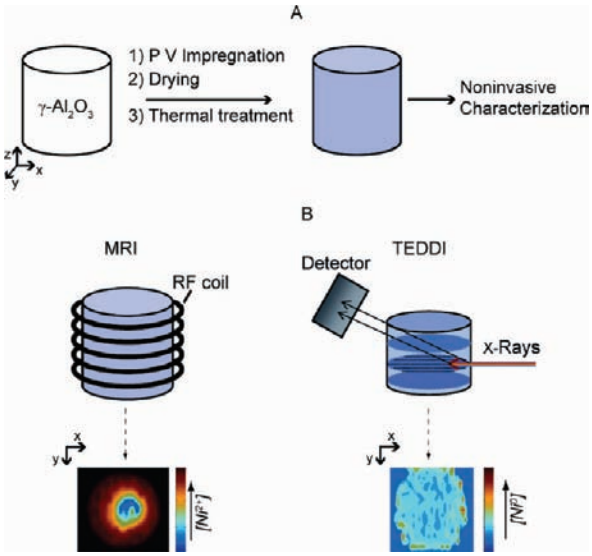

FIGURE 7. (A) Sample preparation to apply noninvasive characterization techniques during the impregnation, drying, or thermal treatment steps of a catalyst body and (B) characterization approach of the MRI and TEDDI techniques together with the typical images obtained from them.

from the inside of the samples. One question that arises, especially in the analysis of wet extrudates after impregnation, is whether the processes under investigation are influenced by this bisection. For example, one could expect that bisection brings about modification of the surface due to attrition or rapid drying of the sample under study. Furthermore, an inherent limitation of the pre-bisection of the samples is that the drying or thermal treatment steps cannot be studied in situ. This brings the desire for the development of noninvasive methods that enable in situ characterization of all the steps involved in catalyst preparation. In this direction, one can find techniques such as magnetic resonance imaging (MRI), which provides input in two dimensions (2D) and has been employed, for example, to study the impregnation of different metal-ion precursor complexes or the drying of different support pellets. Another new type of measurement, which also serves to study the pore structure of materials is 2D nuclear magnetic resonance (NMR) relaxation time measurements.[23−26] Additionally, noninvasive synchrotron-based techniques, such as tomographic energy dispersive diffraction imaging (TEDDI) and X-ray microtomography, are under investigation in the field of catalyst preparation.[27−29] Figure 7 illustrates the experimental approach to be followed when the samples are characterized by noninvasive methods.

The MRI image shown in Figure 7B represents an *xy* slice of a γ-Al_2O_3 extrudate 5 min after impregnation with a 0.5 M $Ni(H_2O)_6^{2+}$ solution. The red region indicates a high concentration of the complex, while the blue core indicates the presence of pure water. The TEDDI image in Figure 7B represents an *xy* slice of a Ni/γ-Al_2O_3 pellet after thermal treatment in N_2. A green external ring can be observed, which indicates an egg-shell distribution of the metallic Ni (200) reflection at 57.6 keV.

3.1. Magnetic Resonance Imaging. MRI is a widely used technique in the field of medicine and in the last decades has been used for various applications in material sciences and catalysis.[30,31] To obtain MRI images the catalyst body is placed in the center of a radiofrequency coil and the magnetization of nuclei in a constant magnetic field is manipulated by the application of radiofrequency pulses. By application of specific radiofrequency, phase encoding, and frequency encoding routines, information on the distribution of the nuclei in the *xy* plane of the catalyst body can be obtained in a noninvasive manner.[32] Spatial resolutions used in material sciences and catalysis lie on the order of a few micrometers and are a compromise between signal-to-noise ratio (higher spatial resolution lower signal-to noise ratio) and time resolution required (higher spatial resolution lower time resolution). Additionally, the type of NMR-sensitive nuclei used also affect the spatial resolution of the technique; in this sense the use of nuclei with smaller gyromagnetic ratios (^{13}C compared to ^{1}H) results in a loss of spatial resolution (when the same magnetic field gradients are used). There are several MRI approaches to image the impregnation step or the catalyst bodies after drying.

3.1.1. Indirect Imaging of Paramagnetic and Diamagnetic Species by ^{1}H MRI. The contrast in an NMR (nuclear magnetic resonance) image is a direct measure of the NMR intensity of water protons. This intensity can be made to depend on the proton nuclear spin relaxation times T_1 and T_2.[33] It is known that the relaxation times of a liquid decrease in the presence of dissolved paramagnetic ions. Based on this phenomenon, a suitable T_1 or T_2 contrast can be chosen to visualize the regions in a catalyst body with and without paramagnetic species. To image, for example, the dynamics of aqueous paramagnetic metal-ion complexes after incipient wetness impregnation, one can apply T_2 contrast and the diffusion of the complex can be clearly visualized, as illustrated in Figure 8. By application of T_2 contrast, the NMR signal coming from regions where Ni^{2+} (or other paramagnetic species) is present is suppressed.

Figure 8B shows the ^{1}H MRI images of an Al_2O_3 body at several times after incipient wetness impregnation with a 0.5 M aqueous $Ni(NO_3)_2$ solution.[24] A quantitative plot of $Ni(H_2O)_6^{2+}$ distribution as a function of time is also presented in Figure 8A. As deduced from the Figure, 60 min was neces-

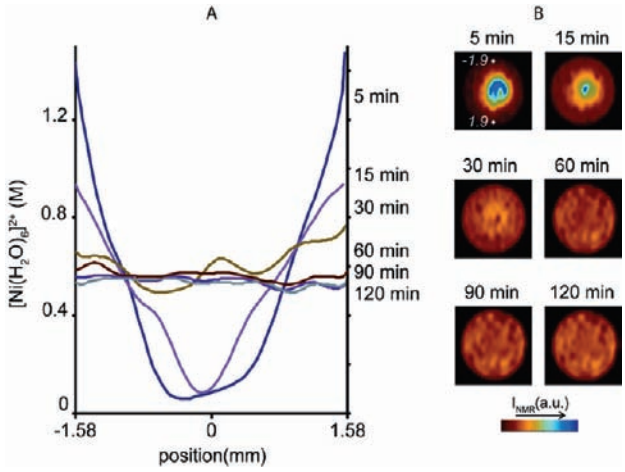

FIGURE 8. (A) One-dimensional profiles of the $Ni(H_2O)_6^{2+}$ concentration as a function of the position inside the extrudates at certain times after impregnation of an aqueous 0.5 M $Ni(H_2O)_6^{2+}$ solution; (B) NMR images recorded after impregnation of the same solution (spatial resolution 231 μm $\times$ 139 μm). The red-colored areas represent high $Ni(H_2O)_6^{2+}$ concentrations and the blue colored areas represent low concentrations of the same complex.[24]

sary to achieve a Ni^{2+} uniform distribution along the catalyst body, and from the concentration profiles, the diffusion could be followed in a quantitative manner. This quantitative approach has also been used to study the dynamics of other paramagnetic metal-ion complexes such as $Co(H_2O)_6^{2+}$ and $Cu(H_2O)_6^{2+}$, proving its general validity.[23,34] T_2 contrast can also be used to visualize the dynamics of other complexes in which the paramagnetic metal ion is surrounded by ligands different from water, for example, Co^{2+}–citrate complexes.[35]

By use of T_1 contrast, the dynamics of complexes that have a weak influence on the relaxation times of water protons can be monitored. One example is the dynamics of $Ni(edta)^{2-}$ in an Al_2O_3 catalyst body.[18] Due to the bulkiness of this ligand, the water protons do not feel the presence of Ni^{2+} and T_2 contrast cannot be used. The main disadvantage of applying T_1 contrast is that the MRI images obtained are not quantifiable. Hence, this method is purely qualitative.

The dynamics of diamagnetic species can also be imaged by adding an inversion recovery pulse sequence to the MRI experiment.[32] An example published by Koptyug and co-workers[34] illustrates the diffusion of $Mo_7O_{24}^{6-}$ anions inside an Al_2O_3 body after impregnation of a 2 M aqueous solution of ammonium heptamolybdate at pH 5.5. Moreover, the location of other compounds interesting in the design of catalysts, such as citrate, can also be visualized using the inversion recovery preconditioning.[34]

Additionally, the ^{1}H MRI approach can be utilized to study the location of both paramagnetic and diamagnetic species in catalyst bodies after drying. To do so, the sample after impregnation and drying must be saturated with a nonpolar liquid such as cyclohexane and the ^{1}H NMR images are collected using T_1 or T_2 contrast or the inversion recovery preconditioning.[34]

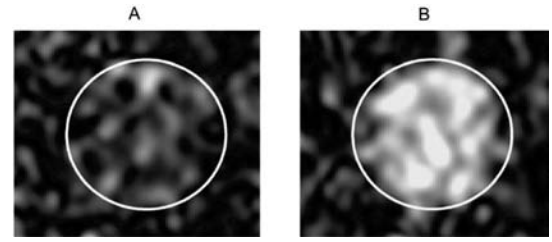

FIGURE 9. ^{13}C NMR images (spatial resolution 270 μm $\times$ 292 μm) of Al_2O_3 catalyst bodies 40 min after impregnation of a 0.4 M ^{13}C-labeled citrate solution at (A) pH 1 and (B) pH 9. The white circle represents the contour of the catalyst body and the regions in white represent high ^{13}C NMR signal.[34]

3.1.2. Direct Imaging of NMR-Sensitive Nuclei. MRI can be used to directly detect the signal coming from the precursor of the active phase, as for ^{195}Pt, or the signal coming from other additives such as organic molecules (^{13}C) or phosphates (^{31}P). An example is the use of ^{13}C MRI to locate citric acid after its impregnation on an Al_2O_3 body.[34] Figure 10 shows the ^{13}C NMR images obtained after impregnation of a 0.4 M aqueous solution of 1,5-^{13}C-labeled citric acid.

The image obtained after impregnation with a citric acid solution at pH 1 illustrated in Figure 9A shows no NMR signal; that is, it is not possible to distinguish citric acid. This is caused by the strong adsorption of citrate at pH 1 on the walls of Al_2O_3 resulting in a loss of mobility of citrate molecules and a consequent reduction in the T_2 relaxation times. On the other hand, at pH 9 citrate does not adsorb strongly on the Al_2O_3 walls and moves toward the core of the body giving rise to a uniform profile 40 min after impregnation, as illustrated in Figure 9B.

These examples demonstrate the potential of MRI to gain insight into the dynamics of the different components of an impregnation solution in a catalyst body. Additionally, it can be used as a camera to locate different components after drying. Hence, the combination of this technique with other space-resolved techniques can yield fundamental knowledge on the processes talking place in a catalyst body during preparation.

3.2. Tomographic Energy Dispersive Diffraction Imaging. Tomographic energy dispersive diffraction imaging (TEDDI) is a recently developed synchrotron-based characterization method that uses a synchrotron beam to obtain three-dimensional (3D) information on the elemental composition and related crystalline phases of the interior of a material in a noninvasive manner. The scanned volume of the material

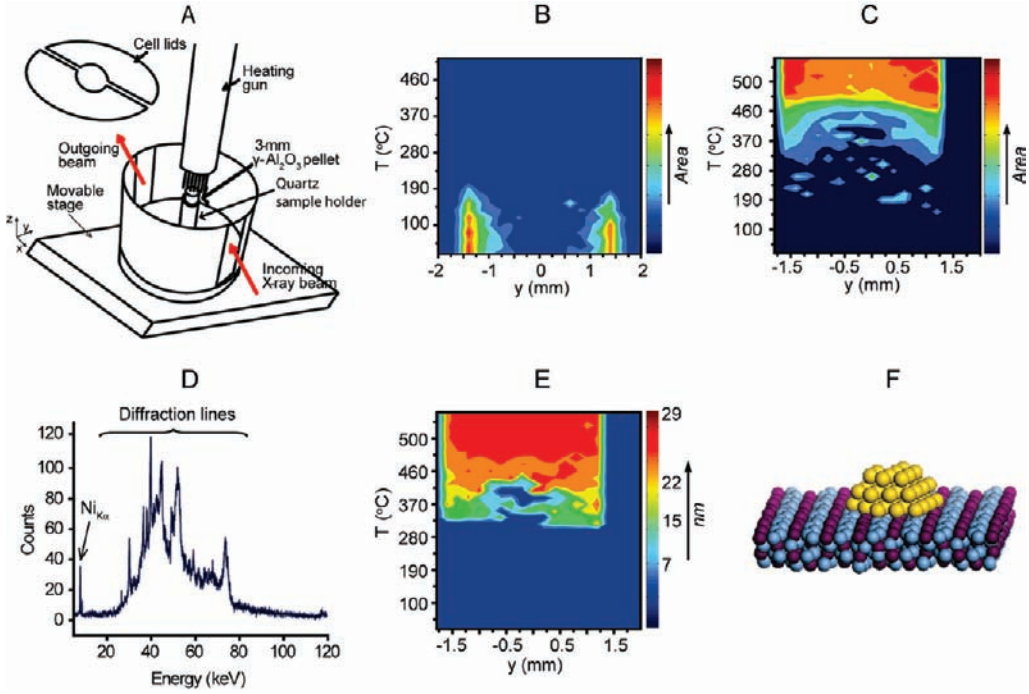

FIGURE 10. (A) Schematic of the environmental cell designed for in situ calcination TEDDI experiments; (D) Detector signal from a Ni/Al_2O_3 catalyst body after drying at 20 °C; 1D *y* scan lines as a function of temperature during the calcination in N_2 of Ni/Al_2O_3 catalyst bodies, constructed from (B) diffraction peak at 39.3 keV of $Ni(en)_3(NO_3)_2$, (C) diffraction peak at 57.6 keV of fcc metallic Ni obtained after impregnation and drying of $Ni(en)(H_2O)_4Cl_2/Al_2O_3$, and (E) growth of metallic Ni crystallites obtained from the map depicted in panel C; (F) Illustration of a Ni^0 particle on Al_2O_3.[36]

comes from the cross-section between the incoming X-ray beam and the scattered X-ray beam at a fixed angle and has a size of $2.47 \times 0.1 \times 0.2$ mm^3 ($x \times y \times z$), which corresponds to the spatial resolution of the experimental setup. This cross-section is fixed during the TEDDI experiments, and by means of a movable (x, y, z) stage, the sample is moved toward or away from it enabling one to obtain information at infinite locations of the sample.[36] The selection of the scanned volume size in the y and z directions is a compromise between space and time resolution. Currently, up to few hours are required to obtain a 2D TEDDI image such as the ones presented in Figure 10, and this time scale can only be improved either by using brighter X-ray sources or by upgrading the detection system.[37,38]

This technique can be applied to profile the sample after drying or calcination or during the heating process thanks to the environmental cell presented in Figure 10A, which permits temperature and gas environment control of the system during measurements. Figure 10 additionally presents the application of in situ TEDDI during the calcination in N_2 of two Ni/Al_2O_3 hydrogenation catalyst bodies prepared from two different precursor complexes: $[Ni(en)_3](NO_3)_2$ and $[Ni(en)(H_2O)_4]Cl_2$.[36] During the measurements a typical spectrum such as that illustrated in Figure 10D is collected for every scanned volume. This spectrum corresponds to a $Ni(en)_3^{2+}/Al_2O_3$ catalyst body after drying in the edge. A number of peaks can be identified in this spectrum due to the fluorescence of Ni at around 7.5 keV ($Ni_{K\alpha}$) and due to the diffraction of $[Ni(en)_3](NO_3)_2$ and γ-Al_2O_3, providing information of both elemental and crystalline-phase distribution. By scanning the y direction as a function of the temperature, one can construct maps such as the one depicted in Figure 10B. A red color in the maps indicates a high number of counts reaching the detector and a high concentration of the species of interest. The map in Figure 10B was calculated from the diffraction peak at 39.3 keV of crystalline $Ni(en)_3(NO_3)_2$, which was formed during drying and indicates an egg-shell distribution of the Ni precursor salt. The decomposition of the precursor salt takes place at around 190 °C to yield an amorphous Ni phase that finally transformed partly into metallic Ni nanoparticles of around 5 nm.[36]

The formation of metallic Ni from $Ni(en)(H_2O)_4Cl_2$ on an Al_2O_3 catalyst body during calcination and estimated from a peak at 57.6 keV is presented in Figure 10C.[36] Metallic Ni (fcc) crystals form first in the edges at around 350 °C, and the growth front moves toward the core of the body at 460 °C, as deduced from the figure. From the peak shape at 57.6 keV, an estimation of the particle size growth can be done and is

presented in Figure 10E. At 500 °C, the average particle size of metallic Ni was calculated to be 26 nm. This value was not far away from the particle size estimation done by TEM (transmission electron microscopy).[36]

TEDDI has revealed that the formation of an active component is a multistep evolution process and that this process shows significant spatial variation. Important is the fact that this technique is the first one that can be used to characterize drying steps in an in situ manner. It is fair to say, on the other hand, that the measuring time to collect a full map is still in the order of hours with the consequent loss of information between scans.

4. Future Prospects

Since the preparation of the optimum catalyst is based on a multidisciplinary approach that involves knowledge from several research fields (interfacial chemistry, spectroscopy, analytical chemistry, physical chemistry, and material sciences) the development of space- and time-resolved spectroscopic techniques brings new tools that are of interest for scientists in a wide range of fields and applications, from medical engineering (development of biomaterials) to civil engineering (e.g., structure of concretes). Moreover, with the help of these methods, enormous value can be gained by the chemical industry due to the current need in our society for sustainable development.

As further developments of the techniques currently in use, one can think of the importance to increase the spatial resolution of the methods so a perfect location of the active particle and its molecular structure can be achieved. Moreover, an increase in time resolution of techniques such as TEDDI will unravel the presence of potential intermediate phases during catalyst preparation, making it possible to apply these techniques during real catalytic processes. In this regard, new approaches such as multitechnique mapping or wide-field X-ray imaging, both of which utilize synchrotron radiation, seem to be the most promising.[39,40] An increase in chemical sensitivity is also desired in the particular case of MRI, with which the direct imaging of NMR-sensitive nuclei is limited by the natural abundance and gyromagnetic ratio of the NMR-active isotopes. Thus, improvements in the equipment and acquisition method can bring about higher chemical and spatial sensitivity. Very important is the possibility of utilizing these techniques in a quantitative and time-resolved manner for modeling the kinetics of all time-dependent processes. Furthermore, there are other catalyst preparation methods that are also used for industrial applications as well as at laboratory scale. These methods include CVD (chemical vapor deposition), HDP (homogeneous deposition precipitation), or wet impregnation. It would be interesting to design methodologies that would allow the study of catalyst preparation regardless the preparation method. Finally, in the design of efficient catalyst bodies, the influence that the 3D network of the pore structure of a support body has on the dynamics of the precursor complex and growth and formation of the active component cannot be neglected. These three are determined not only by the number and type of surface adsorption sites but also by the pore structure, namely, tortuosity of the pores, pore diameter, and pore size distribution. Thus, the shaping of support bodies is also important. In this regard, not much attention has been paid for the moment to the effect that the 3D pore structure of the support body has on the genesis of the active component, and only a few studies on the characterization of preshaped supports have been published.[28−30] Techniques that show great potential in this area are synchrotron-based and research is being carried out in this direction.

The authors acknowledge financial support by the Dutch National Science Foundation (NWO-CW, NRSCC, and ASPECT-ACTS). The following people have contributed to this work: J. A. Bergwerff, L. G. van de Water, M. G. O'Brien, T. A. Nijhuis, T. Visser, K. P. de Jong (Utrecht University); A. A. Lysova, I. V. Koptyug (ITC, Novosibirsk); S. D. M. Jacques, T. Sochi, and P. Barnes (UCL, United Kingdom).

BIOGRAPHICAL INFORMATION

Leticia Espinosa-Alonso was born in León (Spain) on November 3, 1981. She graduated in Chemistry at Universidad Complutense de Madrid (Spain) in 2005. She received her Ph.D. degree in 2009 from Utrecht University, the Netherlands. Her thesis, supervised by Prof. Weckhuysen and Prof. de Jong, was entitled "Space and Time Resolved Spectroscopy during the Preparation of Hydrogenation Catalyst Bodies". Currently she is working as a postdoctoral researcher in the Catalysis Engineering group at Delft University of Technology (the Netherlands).

Andrew M. Beale was born in Beckenham (U.K.) on October 14, 1974. He earned his Ph.D. at University College London in 2002 under supervision of Profs. Sankar and Catlow. After working as a postdoctoral researcher with Prof. Weckhuysen, he became assistant professor in the same group, focusing on the application of scattering and spectroscopic methods for catalyst characterization.

Bert M. Weckhuysen, born in Aarschot (Belgium) on July 27, 1968, is Professor of Inorganic Chemistry and Catalysis at Utrecht University. His research focuses on the potential of spectroscopy of heterogeneous catalysts during catalyst preparation and real operation conditions. After obtaining his Ph.D. from Leuven

University in 1995 under supervision of Prof. Schoonheydt, he worked as a postdoctoral researcher with Prof. Wachs at Lehigh University (Pennsylvania, U.S.A.) and with Prof. Lunsford at Texas A&M University (Texas, USA).

FOOTNOTES

*To whom correspondence should be addressed. e-mail: b.m.weckhuysen@uu.nl.

REFERENCES

1 *Synthesis of Solid Catalysts*; de Jong, K. P., Ed.; Wiley-VCH: Weinheim, Germany, 2009.

2 Neimark, A. V.; Kheifets, L. I.; Fenelonov, V. B. Theory of Preparation of Supported Catalysts. *Ind. Eng. Chem. Prod. Res. Dev.* **1981**, *20*, 439–450.

3 Iglesia, E.; Soled, S. L.; Baumgartner, J. E.; Reyes, S. C. Synthesis and Catalytic Properties of Eggshell Cobalt Catalysts for the Fischer−Tropsch Synthesis. *J. Catal.* **1995**, *153*, 108–122.

4 Kunimori, K.; Nakajima, I.; Uchijima, T. Catalytic Performance of Eggwhite Type Pt/Al_2O_3 Catalyst in the Oxidation of C_3H_8 and CO. *Chem. Lett.* **1982**, *11*, 1165–1168.

5 Minhas, S.; Carberry, J. J. On the Merits of Partially Impregnated Catalysts. *J. Catal.* **1969**, *14*, 270–272.

6 Summers, J. C.; Ausen, S. A. Catalyst Impregnation: Reactions of Noble Metal Complexes with Alumina. *J. Catal.* **1978**, *52*, 445–452.

7 Liu, X.; Khinast, J. G.; Glasser, B. J. A Parametric Investigation of Impregnation and Drying of Supported Catalysts. *Chem. Eng. Sci.* **2008**, *63*, 4517–4530.

8 van Dillen, A. J.; Terörde, R. J. A. M.; Lensveld, D. J.; Geus, J. W.; de Jong, K. P. Synthesis of Supported Catalysts by Impregnation and Drying Using Aqueous Chelated Metal Complexes. *J. Catal.* **2003**, *216*, 257–264.

9 Negrier, F.; Marceau, E.; Che, M.; Giraudon, J. M.; Gengembre, L.; Lofberg, A. A Systematic Study of the Interactions between Chemical Partners (Metal, Ligands, Counterions, and Support) Involved in the Design of Al_2O_3-Supported Nickel Catalysts from Diamine−Ni(II) Chelates. *J. Phys. Chem. B* **2005**, *109*, 2836–2845.

10 Ryczkowski, J. Modification of Preparation Technique for Highly Dispersed Ni/γ-Al_2O_3 Catalysts. *React. Kinet. Catal. Lett.* **1989**, *40*, 189–194.

11 Sietsma, J. R. A.; Meeldijk, J. D.; Versluijs-Helder, M.; Broersma, A.; Dillen, A. J. v.; de Jongh, P. E.; de Jong, K. P. Ordered Mesoporous Silica To Study the Preparation of Ni/SiO_2 ex Nitrate Catalysts: Impregnation, Drying, and Thermal Treatments. *Chem. Mater.* **2008**, *20*, 2921–2931.

12 Schwarz, J. A.; Heise, M. S. Preparation of Metal Distributions within Catalyst Supports: IV. Multicomponent Effects. *J. Colloid Interface Sci.* **1990**, *135*, 461–467.

13 Carrier, X.; Lambert, J. F.; Che, M. Ligand-Promoted Alumina Dissolution in the Preparation of $MoOx/\gamma$-Al_2O_3 Catalysts: Evidence for the Formation and Deposition of an Anderson-type Alumino Heteropolymolybdate. *J. Am. Chem. Soc.* **1997**, *119*, 10137–10146.

14 Deo, G.; Wachs, I. E. Predicting Molecular Structures of Surface Metal Oxide Species on Oxide Supports under Ambient Conditions. *J. Phys. Chem.* **1991**, *95*, 5889–5895.

15 d'Espinose de la Caillerie, J.-B.; Kermarec, M.; Clause, O. Impregnation of γ-alumina with Ni(II) or Co(II) Ions at Neutral pH: Hydrotalcite-Type Coprecipitate Formation and Characterization. *J. Am. Chem. Soc.* **1995**, *117*, 11471–11481.

16 Bergwerff, J. A.; van de Water, L. G. A.; Visser, T.; de Peinder, P.; Leliveld, B. R. G.; de Jong, K. P.; Weckhuysen, B. M. Spatially Resolved Raman and UV-visible-NIR Spectroscopy on the Preparation of Supported Catalyst Bodies: Controlling the Formation of $H_2PMo_{11}CoO_{40}^{5-}$ inside Al_2O_3 pellets during impregnation. *Chem.—Eur. J.* **2005**, *11*, 4592–4601.

17 Mang, T.; Breitscheidel, B.; Polanek, P.; Knözinger, H. Adsorption of Platinum Complexes on Silica and Alumina: Preparation of Non-uniform Metal Distributions within Support Pellets. *Appl. Catal., A* **1993**, *106*, 239–258.

18 Espinosa-Alonso, L.; de Jong, K. P.; Weckhuysen, B. M. Effect of the Nickel Precursor on the Impregnation and Drying of γ-Al_2O_3 Catalyst Bodies: A UV-vis and IR Microspectroscopic Study. *J. Phys. Chem. C* **2008**, *112*, 7201–7209.

19 Espinosa-Alonso, L.; De Jong, K. P.; Weckhuysen, B. M. A UV-Vis Micro-spectroscopic Study to Rationalize the Influence of Cl^- (aq) on the Formation of Different Pd Macro-distributions on γ-Al_2O_3 Catalyst Bodies. *Phys. Chem. Chem. Phys.* **2010**, *12*, 97–107.

20 van de Water, L. G. A.; Bezemer, G. L.; Bergwerff, J. A.; Versluijs-Helder, M.; Weckhuysen, B. M.; de Jong, K. P. Spatially Resolved UV-Vis Microspectroscopy on the Preparation of Alumina-supported Co Fischer−Tropsch Catalysts: Linking Activity to Co Distribution and Speciation. *J. Catal.* **2006**, *242*, 287–298.

21 Lever, A. B. P. *Inorganic Electronic Spectroscopy*; Elsevier Science B. V.: Amsterdam, 1987.

22 Bergwerff, J. A.; Jansen, M.; Leliveld, B. G.; Visser, T.; de Jong, K. P.; Weckhuysen, B. M. Influence of the Preparation Method on the Hydrotreating activity of MoS_2/Al_2O_3 Extrudates: A Raman Microspectroscopy Study on the Genesis of the Active Phase. *J. Catal.* **2006**, *243*, 292–302.

23 Bergwerff, J. A.; Lysova, A. A.; Espinosa Alonso, L.; Koptyug, I. V.; Weckhuysen, B. M. Probing the Transport of Paramagnetic Complexes Inside Catalyst Bodies in a Quantitative Manner by Magnetic Resonance Imaging. *Angew. Chem., Int. Ed.* **2007**, *46*, 7224–7227.

24 Espinosa-Alonso, L.; Lysova, A. A.; de Peinder, P.; de Jong, K. P.; Koptyug, I. V.; Weckhuysen, B. M. Magnetic Resonance Imaging Studies on Catalyst Impregnation Processes: Discriminating Metal Ion Complexes within Millimeter-Sized γ-Al_2O_3 Catalyst Bodies. *J. Am. Chem. Soc.* **2009**, *131*, 6525–6534.

25 Koptyug, I. V.; Fenelonov, V. B.; Khitrina, L. Y.; Sagdeev, R. Z.; Parmon, V. N. In Situ NMR Imaging Studies of the Drying Kinetics of Porous Catalyst Support Pellets. *J. Phys. Chem. B* **1998**, *102*, 3090–3098.

26 Mitchell, J.; Chandrasekera, T. C.; Johns, M. L.; Gladden, L. F.; Fordham, E. J. Nuclear Magnetic Resonance Relaxation and Diffusion in the Presence of Internal Gradients: The Effect of Magnetic Field Strength. *Phys. Rev. E* **2010**, *81*, 026101.

27 Beale, A. M.; Jacques, S. D. M.; Bergwerff, J. A.; Barnes, P.; Weckhuysen, B. M. Tomographic Energy Dispersive Diffraction Imaging as a Tool To Profile in Three Dimensions the Distribution and Composition of Metal Oxide Species in Catalyst Bodies. *Angew. Chem., Int. Ed.* **2007**, *46*, 8832–8835.

28 Grunwaldt, J.-D.; Kimmerle, B.; Baiker, A.; Boye, P.; Schroer, C. G.; Glatzel, P.; Borca, C. N.; Beckmann, F. Catalysts at Work: From Integral to Spatially Resolved X-ray Absorption Spectroscopy. *Catal. Today* **2009**, *145*, 267–278.

29 Ruffino, L.; Mann, R.; Oldman, R.; Stitt, E. H.; Boller, E.; Cloetens, P.; Di Michiel, M.; Merino, J. Using X-Ray Microtomogaphy for Characterisation of Catalyst Particle Pore Structure. *Can. J. Chem. Eng.* **2005**, *83*, 132–139.

30 Hollewand, M. P.; Gladden, L. F. Heterogeneities in Structure and Diffusion within Porous Catalyst Support Pellets Observed by NMR Imaging. *J. Catal.* **1993**, *144*, 254–272.

31 Koptyug, I. V.; Lysova, A. A.; Matveev, A. V.; Parmon, V. N.; Sagdeev, R. Z. NMR Imaging of Mass Transport Processes and Catalytic Reactions. *Top. Catal.* **2005**, *32*, 83–91.

32 Callaghan, P. T. *Principles of Nuclear Magnetic Resonance Microscopy*; Claredon Press: Oxford, U.K., 1991.

33 Lauffer, R. B. Paramagnetic Metal complexes as Water Proton Relaxation Agents for NMR Imaging: Theory and Design. *Chem. Rev.* **1987**, *87*, 901–927.

34 Lysova, A. A.; Bergwerff, J. A.; Espinosa-Alonso, L.; Weckhuysen, B. M.; Koptyug, I. V. Magnetic Resonance Imaging as an Emerging Tool for Studying the Preparation of Supported Catalysts. *Appl. Catal., A* **2010**, *374*, 126–136.

35 Bergwerff, J. A.; Lysova, A. A.; Espinosa-Alonso, L.; Koptyug, I. V.; Weckhuysen, B. M. Monitoring Transport Phenomena of Paramagnetic Metal-ion Complexes Inside Catalyst Bodies with Magnetic Resonance Imaging. *Chem.—Eur. J.* **2008**, *14*, 2363–2374.

36 Espinosa-Alonso, L.; O'Brien, M. G.; Jacques, S. D. M.; Beale, A. M.; de Jong, K. P.; Barnes, P.; Weckhuysen, B. M. Tomographic Energy Dispersive Diffraction Imaging To Study the Genesis of Ni Nanoparticles in 3D within γ-Al_2O_3 Catalyst Bodies. *J. Am. Chem. Soc.* **2009**, *131*, 16932–16938.

37 Cernik, R. J.; Khor, K. H.; Hansson, C. X-Ray Colour Imaging. *J. R. Soc. Interface* **2008**, *5*, 477–481.

38 Middelkoop, V.; Boldrin, P.; Peel, M.; Buslaps, T.; Barnes, P.; Darr, J. A.; Jacques, S. D. M. Imaging the Inside of a Continuous Nanoceramic Synthesizer Under Supercritical Water Conditions Using High-Energy Synchrotron X-Radiation. *Chem. Mater.* **2009**, *21*, 2430–2435.

39 Kimmerle, B.; Grunwaldt, J.-D.; Baiker, A.; Glatzel, P.; Boye, P.; Stephan, S.; Schroer, C. G. Visualizing a Catalyst at Work During the Ignition of the Catalytic Partial Oxidation of Methane. *J. Phys. Chem. C* **2009**, *113*, 3037–3040.

40 O'Brien, M. G.; Beale, A. M.; Jacques, S. D. M.; Di Michiel, M.; Weckhuysen, B. M. Spatiotemporal Multitechnique Imaging of a Catalytic Solid in Action: Phase Variation and Volatilization During Molybdenum Oxide Reduction. *ChemCatChem* **2009**, *1*, 99–102.